Transactions of the SMiRT 27
Yokohama, Japan, March 3-8, 2024
DivisionⅢ

NUMERICAL STUDY OF PROJECTILE IMPACTS ON STEEL PLATE REINFORCED CONCRETEUSING FEM TO SPH ADAPTIVE METHOD

Hiroki Arai[1], Masafumi Kawabata[2], Miyako Kuwamura[3], Kunio Takekoshi[4] and Kazukuni Niwa[5]

[1] Engineer, Terrabyte Co., Ltd., Tokyo, Japan (hiroki.arai@terrabyte.co.jp)
[2] Senior Manager, Terrabyte Co., Ltd., Tokyo, Japan (masafumi.kawabata@terrabyte.co.jp)
[3] Assistant Manager, Terrabyte Co., Ltd., Tokyo, Japan (miyako.kuwamura@terrabyte.co.jp)
[4] Division Manager, Terrabyte Co., Ltd., Tokyo, Japan (kunio.takekoshi@terrabyte.co.jp)
[5] General Manager, Terrabyte Co., Ltd., Tokyo, Japan (niwa@terrabyte.co.jp)

ABSTRACT

In the finite element (FE) analysis of aircraft impact on steel plate reinforced concrete (SC) structures, scabbing or perforation of concrete is generally modelled by element deletion. Therefore, the analysis ignores the transfer of impact force due to concrete debris to the rear-face steel plate. A solution of the above problem is to replace FE solid elements that have reached failure criteria with smoothed particle hydrodynamics (SPH) or discrete elements. This method allows to model the dispersion of debris after the concrete fractured, and to consider the transfer of impact forces from debris to steel plates. It is also possible to account for the reduction in stiffness of the material after the concrete has been crushed. To validate the proposed modelling methods, comparison between the numerical results using this method and the experimental results of projectile impact tests on SC structures has been carried out. Perforation of a SC panel can be simulated with FE analysis considering the impact forces of concrete debris modelled as SPH elements emerged from deleted concrete solid elements.

INTRODUCTION

Research related to the evaluation of impact strength of critical structures such as nuclear facilities is underway. SC has been reported to have improved impact strength compared to conventional reinforced concrete (RC). In the analysis of aircraft impact on reinforced concrete structures, scabbing or perforation of concrete is generally modelled by element deletion (erosion) (Kadoguchi et al., 2009) or using SPH (Sonoda et al., 2009). When the element deletion method is applied to SC structures, the element erosion technique ignores the transfer of impact force of concrete debris to the rear-face steel plate. A proposed method for the above problem is to replace deleted FE solid elements with SPH or discrete elements.

In this study, the projectile impact analyses using the FE method have been carried out based on the experimental results of a 1/7.5 scale aircraft model impact test (Mizuno et al., 2005). The applicability and effectiveness of the method using SPH for impact failure assessment of the rear-face steel plate considering concrete failure debris are investigated and demonstrated.

ANALYSIS MODEL

Analysis conditions

A structure with steel plates on both sides of the concrete (Full SC, hereafter FSC) and a structure with steel plates only on the rear-face of the concrete (Half SC, hereafter HSC) are considered. The FE model of the FSC is shown in Figure 1: the FSC plate is 110 cm per side and fully fixed on all sides. The concrete and steel plates are connected by studs. The projectile is allowed to impact the SC plate at 150 m/sec.

In the conversion method from Solid to SPH (hereafter referred to as Solid2SPH), the solid elements reached to failure criteria are deleted, but by converting SPH the mass and the momentum are conservated.

In order to perform the analysis with a high degree of accuracy, each solid element is converted into 3 x 3 x 3 = 27 SPHs. The initial tangent modulus of the SPHs for concrete debris part is reduced because concrete that reaches the failure criterion is in a damaged state and is set to 1/1000 of concrete to be consistent with the experimental results.

The projectile impact analyses have been carried out using LS-DYNA to compare the residual velocity of the projectile, displacement of the rear-face steel plate and perforation behaviour with the experimental results.

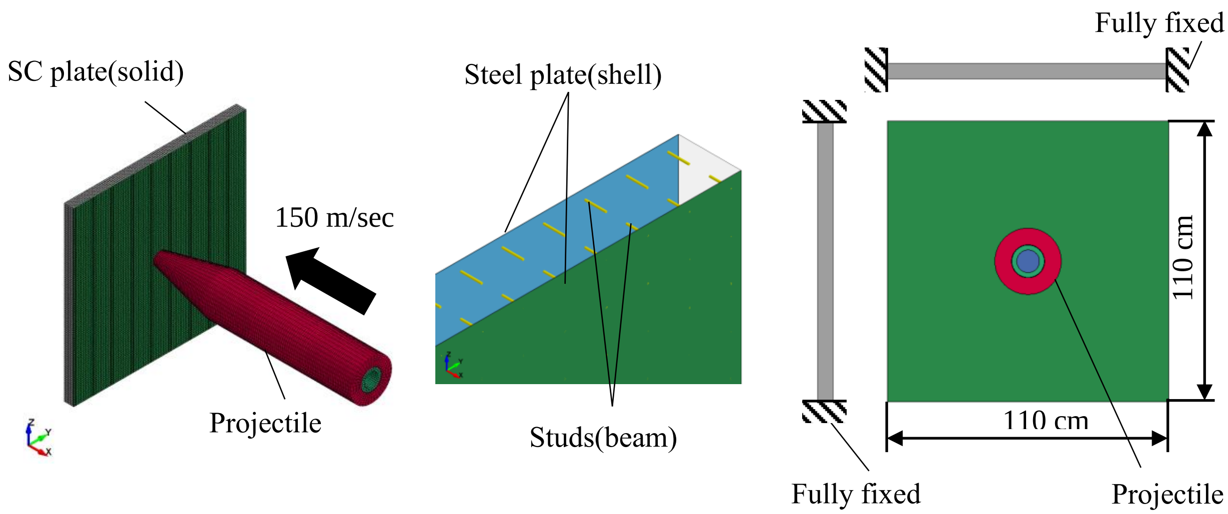

Figure 1. FE model (FSC)

Projectile

A cross-sectional view of the FE model of the projectile (Korematsu et al., 2022) considered in the analyses is shown in Figure 2. The model is designed to predict the peak load of 570 kN reported (Mizuno et al., 2005). The fuselage is made of foam and covered with fibre glass skin. The part equivalent to the engine in the actual aircraft consists of a honeycomb core and a steel outer shell.

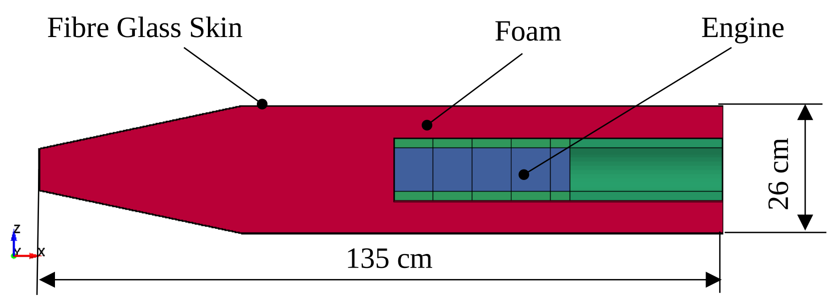

Figure 2. Cross-sectional view of the FE model of the projectile

SC Panels

The concrete and steel plate specifications are given in Table 1 and Table 2. The Winfrith model (Broadhouse, 1995) is used as the material constitutive law for concrete. Strain rate dependence of concrete is considered. An elastoplastic material law is used for steel plates, and the strain rate dependence of steel plates is considered using the Cowper-Symonds model (Cowper and Symonds, 1958). The Cowper-Symonds coefficients are adjusted from the yield point data as a function of strain rate based on the Japan Welding Engineering Society's estimated equation (WES, 2017). The equivalent stress-equivalent plastic strain relationship in static state is estimated with the equation proposed by ASME (ASME, 2019) for steel plates is shown in Figure 3.

Table 1: Material properties of concrete

	Input value
Compressive strength [MPa]	39.6
Tensile strength [MPa]	3.76
Initial tangent modulus [MPa]	26800
Fracture energy [N/m]	92.5
Aggregate size [mm]	20

Table 2: Material properties of steel plate

	Input value
Young's modulus [MPa]	206000
Yield point [MPa]	355
Tensile strength [MPa]	476
C (Cowper-Symonds coefficient)	3115
P (Cowper-Symonds coefficient)	5.86
Failure strain	16.5%

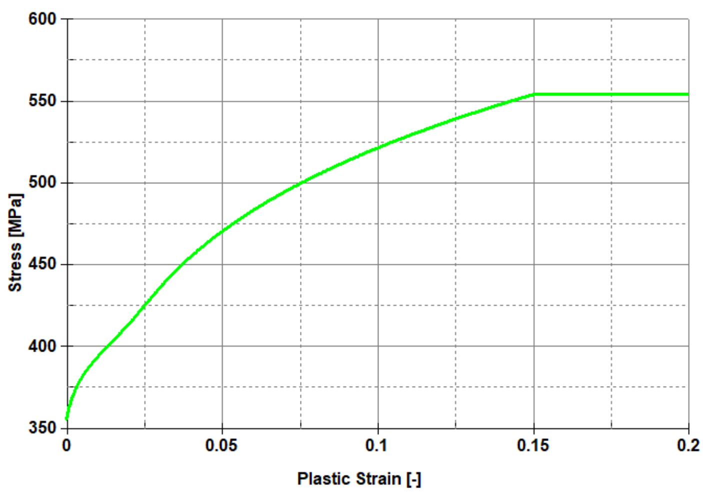

Figure 3. Equivalent stress-equivalent plastic strain relationship for steel plates

RESULTS

Deformation diagram

The results for FSC-60 are shown in Figure 4 as a representative case of perforation; the number following the FSC indicates the concrete plate thickness (mm). In the element deletion method, only the concrete solid elements in the impact zone are deleted. Consequently, the projectile contacts the steel plate directly, it causes to localised bending deformation and leads to rupture in a different process than originally intended; in the Solid2SPH, the impact force is transmitted to the rear-face steel plate by SPH debris, resulting in extensive bending deformation of the steel plate, bulging out and rupture.

The results for FSC-80 are shown in Figure 5 as representative of the non-perforation case. Concrete failure develops in a cone shape from the rear-face. There is the small difference in deformation profile between the element deletion method and the Solid2SPH is small. This is because the impact force is supported by the stiffness of the steel plate when no perforation holes are generated.

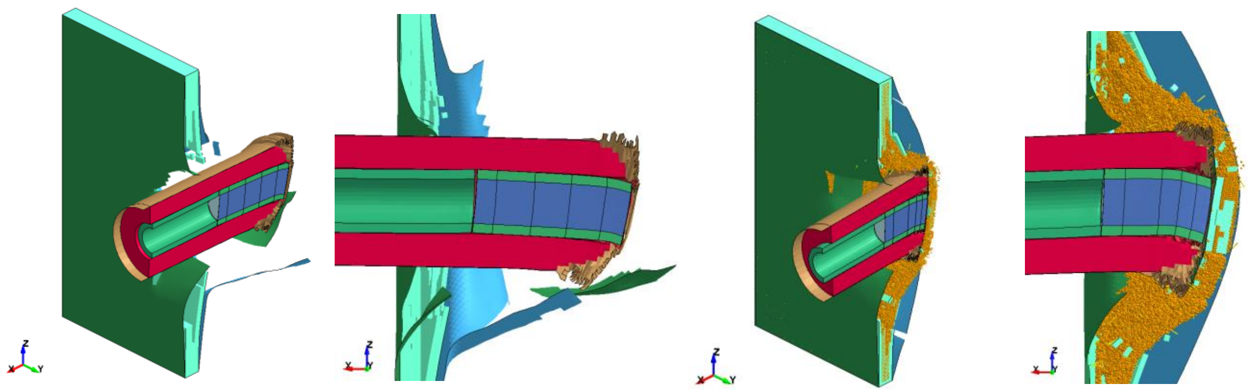

Figure 4. Deformation diagram of FSC-60
Brown particles are converted to SPH debris.
(Left: Element deletion method, right: Solid2SPH)

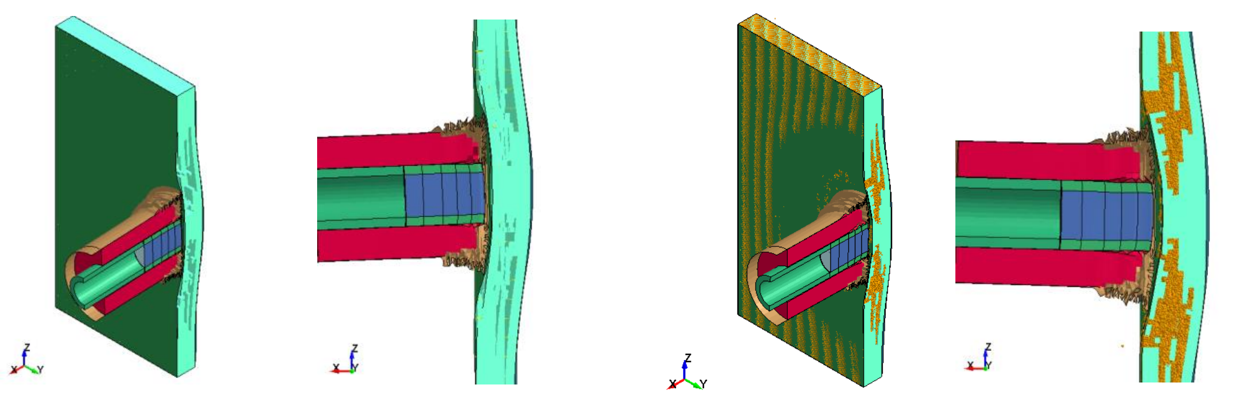

Maximum deformation of the rear steel plate：56 mm　Maximum deformation of the rear steel plate：55 mm

Figure 5. Deformation diagram of FSC-80
Brown particles are converted to SPH debris.
(Left: Element deletion method, right: Solid2SPH)

Velocity history

The time histories of velocity for the projectile evaluated in the experiment and simulation are compared. The comparison results for the FSC-60 are shown in Figure 6. The residual velocity is 28 m/sec for the Solid2SPH and 22 m/sec for the experimental results, which are in almost agreement. The element deletion method results in a residual velocity of 87 m/sec, which is not fully reduced compared to the experiment. In the Solid2SPH, the destructive debris from the SPH contributes to the deceleration of the projectile, and the deceleration and residual velocity are well reproduced.

The projectile velocity history of FSC-80 is shown in Figure 7, which agrees with the experimental results regardless of the conversion to SPH. In this case, the reason why no perforation-holes are formed, and the concrete is less fractured.

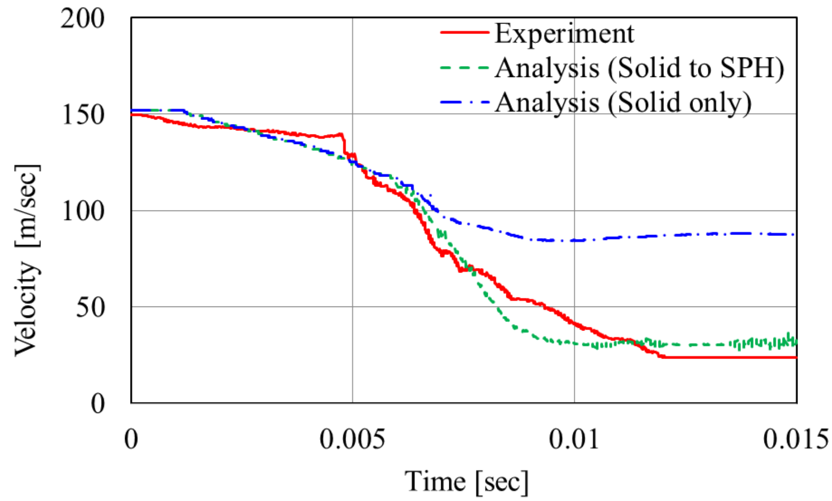

Figure 6. Velocity history of FSC-60

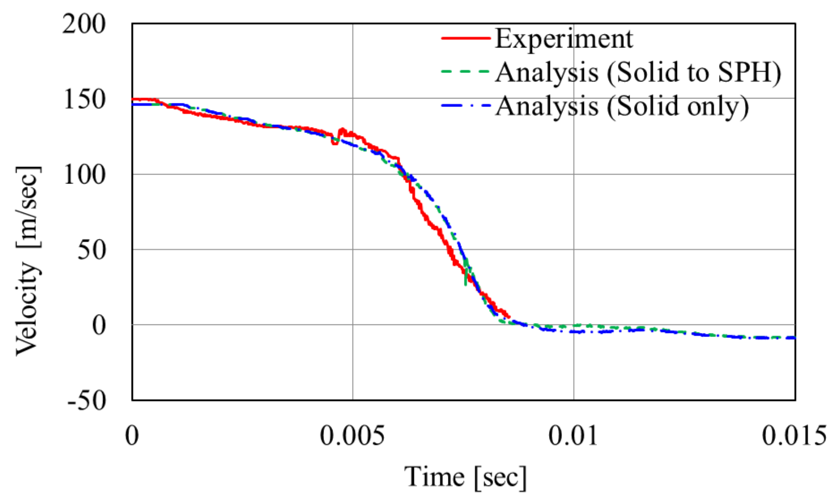

Figure 7. Velocity history of FSC-80

Rupture of the rear-face

The ruptures of the rear-face steel plate of FSC-60 are shown in Figure 8. In the experiment, the studs were dislodged from the 750 mm x 800 mm area on the backside, and the steel plate was teared and pushed out by the projectile and concrete debris. In the case of the element deletion method, the steel plate is teared and pushed out in a narrow area of 630 mm x 630 mm where the projectile contacts directly. In the case of the Solid2SPH, the studs around the projectile are disconnected and the steel plate is teared and pushed out around 850 mm x 750 mm. The Solid2SPH is closer to the experimental results in terms of the size of the rupture area and reproduces the behaviour better.

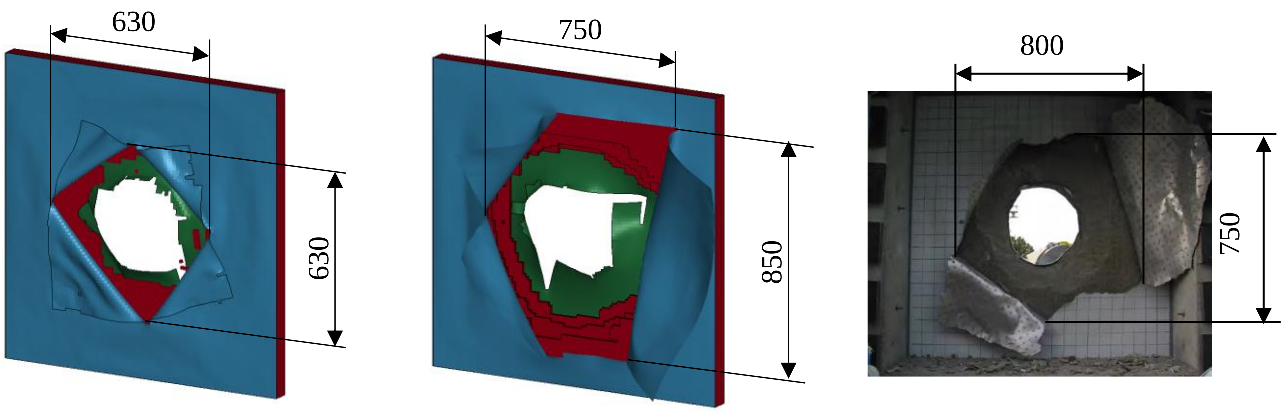

Figure 8. Rupture of rear-face steel plate
(Left: element deletion method, centre: Solid2SPH, right: experimental results)

Debris scattering

To estimate the impact force of the scattered debris, a rigid wall is placed 500 mm behind the rear-face steel plate as shown in Figure 9 and the contact reaction force on the rigid wall is investigated. In the case of the element deletion method, the projectile directly impacts the rigid wall, and the scattering FE debris is compressed immediately after impact and the peak reaction force occurs as shown in Figure 10, The Results of the Solid2SPH are explained as follows, along with the investigation of SPH conversion accuracy.

To confirm the validity of the effect of scattering debris by the Solid2SPH, the results of the comparison of the fracture behaviour are shown between the number of SPHs born from one solid element, 3×3×3 (NQ=3) and 1×1×1 (NQ=1).

The Solid2SPH generates about 1/7 of the reaction force of the element deletion method, with three peaks as shown in Figure 10: at the first peak, debris impact starts, at the second peak, the debris impact area increases, and at the third peak, the projectile load is transmitted through the debris. The maximum value of the reaction force is 300 kN for NQ=3 and 389 kN for NQ=1, with NQ=1 having the earlier onset time of the reaction force; SPHs debris take over mass and kinetic energy from the deleted concrete solid elements, but if the number of SPHs is small, the impact force is difficult to disperse, the rear-face steel plate is more likely to fracture and the impact force of the debris on the rigid wall is also considered to increase.

The perforation-hole diameters are shown in Figure 11: for NQ=3, the diameter of the concrete perforation-hole is 600 mm and the debris impact area on the rigid wall is circular with a diameter of 650 mm; for NQ=1, the diameter of the concrete perforation-hole is 650 mm and the debris impact area on the rigid wall is circular with a diameter of 650 mm. No significant diffusion from the perforation-hole diameter is observed in both cases, with a diffusion angle of 5% for NQ=3 and 0% for NQ=1.

The number of SPHs generated after the removal of concrete solid elements affects impact force on the rigid wall and the diffusion angle of the debris, so the more reliable analysis conditions should be determined by comparison with experimental results.

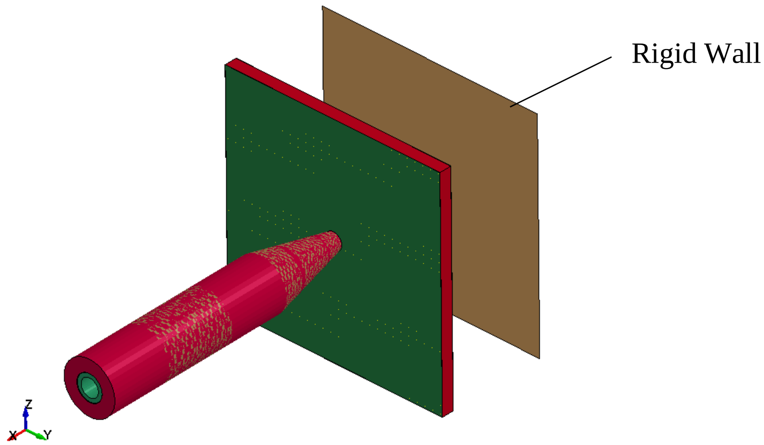

Figure 9. SC Panel and rear rigid wall

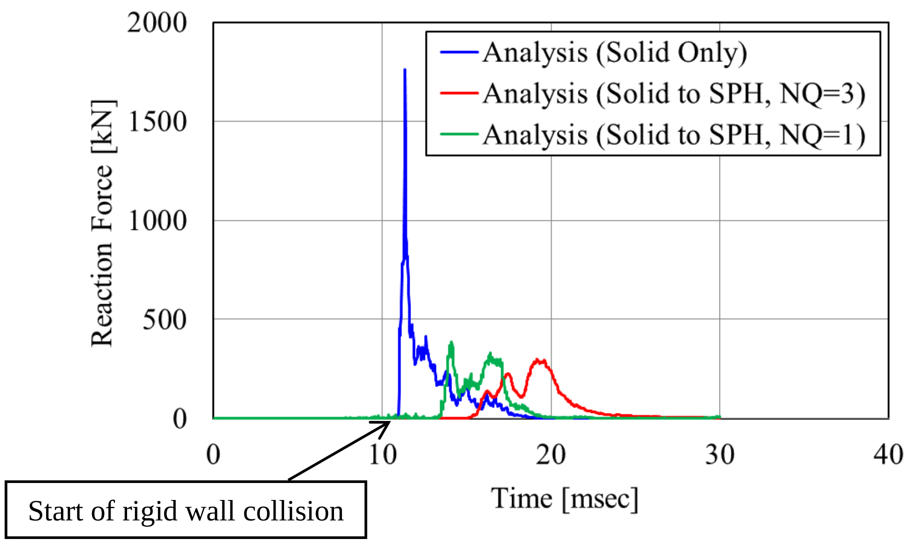

Figure 10. Debris reaction force time history affected to the rear rigid wall

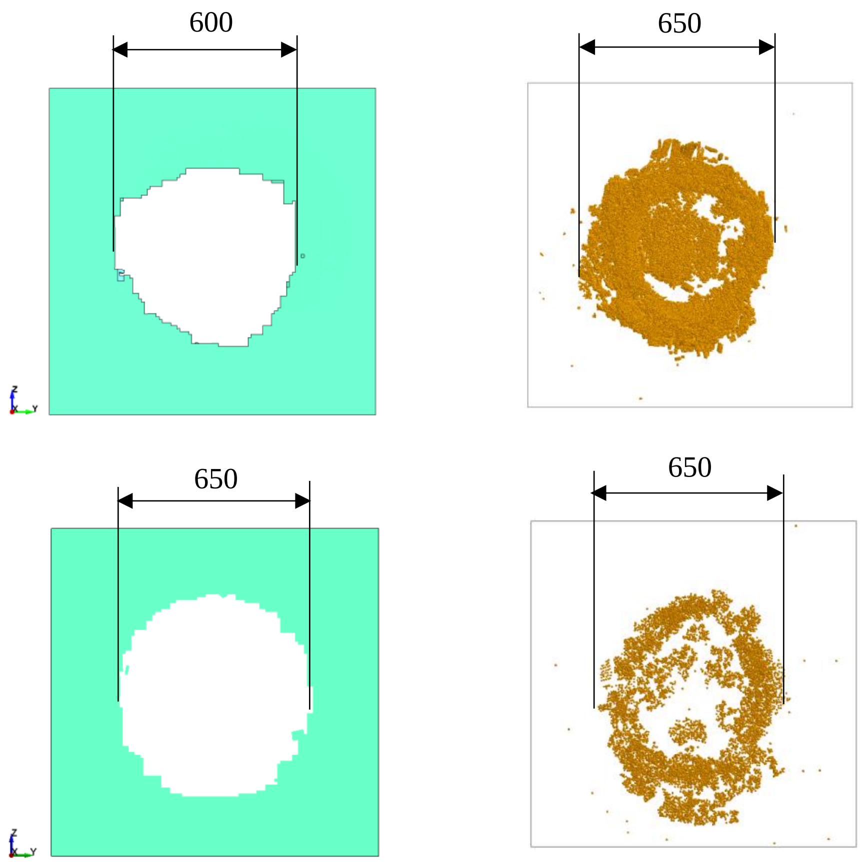

Figure 11. Perforation diameter
Left: perforation, right: debris diffusion, above: NQ = 3, below: NQ = 1

Comparison of simulation and experimental results according to conditions of SC panels

The results of the analysis by the Solid2SPH with the experimental results are compared as shown in Table 3 which include other case of SC panels. In the table, the residual velocity of the projectile and debris, the displacement of the rear steel plate, and the state of perforation and non-perforation are compared with the experiments, and it appears that the simulation results well reproduce the experiments.

Table 3 Comparison of analytical and experimental results using the Solid2SPH

	Residual Velocity of projectile		Residual Velocity of debris		Maximum deformation		Perforation	
	Exp.	Ana.	Exp.	Ana.	Exp.	Ana.	Exp.	Ana.
FSC-60	22	28	58	40	-	-	Perforation	Perforation
HSC-60	40	30	53	35	-	-	Perforation	Perforation
FSC-80	0	0	0	0	43	55	Non-Perforation	Non-Perforation
HSC-80	0	0	0	0	78	91	Non-Perforation	Non-Perforation

CONCLUSION

Based on the 1/7.5 scale aircraft model impact test results, a projectile impact analysis using the finite element method is carried out and the followings are indicated.

(1) The Solid2SPH considering the effect of concrete fracture debris well predicts the residual velocity of the projectile, the fracture aspect and displacement of the rear-face steel plate.
(2) The Solid2SPH is well agreement with the experiment in terms of the residual velocity of projectile and the displacement of the rear-face steel plate, with or without SC perforation.
(3) The Solid2SPH can evaluate the impact force of concrete-fractured debris and the extent of debris diffusion.
(4) As there are differences in the loading history and diffusion behaviour of debris on the back rigid wall depending on the number of SPHs generated, it is necessary to determine the more reliable analysis conditions by comparison with experimental results.

REFERENCES

ASME. (2019). “Boiler and Pressure Vessel Code,” Section VIII, Division2, Annex3-D, US.

Broadhouse, B.J. (1995). “The Winfrith Concrete Model in LS-DYNA3D,” Structural Performance Department, AEA Technology, Winfrith Technology Center, SPD/D (95)363, UK.

Cowper, G. R. and Symonds P. S. (1958). Brown University, Applied Mathematics Report, US.

(General Incorporated association) Japan Welding Society. “Method for evaluating the brittle fracture performance of welded steel structures subjected to dynamic cyclic large deformation (WES2808:2017)”, JP.

Kadoguchi, T. and Niwa, K. (2009. 10). “A study of FE simulation models with perforation for evaluating the strength of RC plates by impact load,” *Proc., 22nd Computational Mechanics Conference*, JP.

Korematsu, T., Murofushi T., Yabuuchi, K. and Kono, Y. (2022). “Experimental study on resistance of steel plate reinforced concrete against projectile impact,” *26th International Conference on Structural Mechanics in Reactor Technology (SMiRT26)*, DE.

Mizuno, J., Sawamoto, Y., Yamashita, T., Koshika N., Niwa, N. and Suzuki A. (2005). “Investigation on impact resistance of steel plate reinforced concrete barriers against aircraft impact Part1: Test Program and Results.”, *18th international Conference on Structural Mechanics in Reactor Technology (SMiRT18)*, CN, 2566-2579.

Mizuno, J., Sawamoto, Y., Yamashita, T., Koshika N., Niwa, N. and Suzuki A. (2005). “Investigation on impact resistance of steel plate reinforced concrete barriers against aircraft impact Part2: Simulation Analysis of scale model impact tests.”, *18th international Conference on Structural Mechanics in Reactor Technology (SMiRT18)*, CN, 2580-2590.

Sonoda, Y. and Goto, W. (2017. 3). “A fundamental study on the impact penetration failure of a concrete slab using SPH method,” *Journal of structural engineering Vol. 63A*, JP.